Cell Reports
Report

Widespread Mitochondrial Depletion via Mitophagy Does Not Compromise Necroptosis

Stephen W.G. Tait,[1,10,*] Andrew Oberst,[2,10] Giovanni Quarato,[3,10] Sandra Milasta,[3] Martina Haller,[1] Ruoning Wang,[4] Maria Karvela,[1] Gabriel Ichim,[1] Nader Yatim,[3,5,6] Matthew L. Albert,[5,6] Grahame Kidd,[7] Randall Wakefield,[8] Sharon Frase,[8] Stefan Krautwald,[9] Andreas Linkermann,[9] and Douglas R. Green[3,*]

[1]CR-UK Beatson Institute, Institute of Cancer Sciences, University of Glasgow, Switchback Road, Glasgow G61 1BD, UK
[2]Department of Immunology, University of Washington, 750 Republican Street, Seattle, WA 98109, USA
[3]Department of Immunology, St. Jude Children's Research Hospital, 262 Danny Thomas Place, Memphis, TN 38105, USA
[4]Center for Childhood Cancer and Blood Disease, The Research Institute at Nationwide Children's Hospital, Department of Pediatrics, The Ohio State University School of Medicine, 700 Children's Drive, Columbus, OH 43205, USA
[5]Unité d'Immunobiologie des Cellules Dendritiques, Department of Immunology, Institut Pasteur, 25 Rue du Docteur Roux, 75724 Paris, France
[6]INSERM U818, Department of Immunology, Institut Pasteur, 25 Rue du Docteur Roux, 75724 Paris, France
[7]Department of Neurosciences, Lerner Research Institute, Cleveland Clinic, Cleveland, OH 44195, USA
[8]Cell and Tissue Imaging Center, St. Jude Children's Research Hospital, 262 Danny Thomas Place, Memphis, TN 38105, USA
[9]Division of Nephrology and Hypertension, Christian Albrechts University, Kiel 24105, Germany
[10]These authors contributed equally to this work
*Correspondence: stephen.tait@glasgow.ac.uk (S.W.G.T.), douglas.green@stjude.org (D.R.G.)
http://dx.doi.org/10.1016/j.celrep.2013.10.034

SUMMARY

Programmed necrosis (or necroptosis) is a form of cell death triggered by the activation of receptor interacting protein kinase-3 (RIPK3). Several reports have implicated mitochondria and mitochondrial reactive oxygen species (ROS) generation as effectors of RIPK3-dependent cell death. Here, we directly test this idea by employing a method for the specific removal of mitochondria via mitophagy. Mitochondria-deficient cells were resistant to the mitochondrial pathway of apoptosis, but efficiently died via tumor necrosis factor (TNF)-induced, RIPK3-dependent programmed necrosis or as a result of direct oligomerization of RIPK3. Although the ROS scavenger butylated hydroxyanisole (BHA) delayed TNF-induced necroptosis, it had no effect on necroptosis induced by RIPK3 oligomerization. Furthermore, although TNF-induced ROS production was dependent on mitochondria, the inhibition of TNF-induced necroptosis by BHA was observed in mitochondria-depleted cells. Our data indicate that mitochondrial ROS production accompanies, but does not cause, RIPK3-dependent necroptotic cell death.

INTRODUCTION

Apoptosis and programmed necrosis are two functionally linked cell death pathways that can be triggered by ligation of members of the "death receptor" (DR) family of cell surface receptors. Apoptosis is orchestrated by activation of the caspase family of cysteine proteases, whereas programmed necrosis is initiated by the receptor interacting protein kinase (RIPK) family members RIPK1 and RIPK3. Signaling through DRs such as tumor necrosis factor receptor 1 (TNFR1) can lead either to apoptosis through activation of Caspase-8 or to programmed necrosis via RIPK1-RIPK3 signaling (He et al., 2009), and the latter is inhibited by the action of a heterodimer of Caspase-8 and the Caspase-8-like molecule c-FLIP$_L$ (Dillon et al., 2012; Oberst et al., 2011). The signaling events that connect receptor ligation to RIPK3 activation have been extensively studied (Green et al., 2011). In contrast, the mechanisms by which RIPK3 activity leads to cell death are less clear, although several studies have implicated mitochondria as downstream effectors of the process (Vanden Berghe et al., 2010; Wang et al., 2012; Zhang et al., 2009). Several reports have also indicated a requirement for ROS production in the execution of RIPK3-dependent programmed necrosis (Cho et al., 2009; Kim et al., 2007; Lin et al., 2004; Vanden Berghe et al., 2010; Vanlangenakker et al., 2011; Zhang et al., 2009). We sought to directly test the roles of mitochondria and mitochondrial reactive oxygen species (ROS) in necroptosis.

RESULTS

Necroptosis Is Executed Independently of Mitochondrial Permeability Transition

During apoptosis (Goldstein et al., 2000; Marzo et al., 1998) and in some forms of necrosis (Baines et al., 2005), the mitochondrial transmembrane potential ($\Delta\Psi$m) dissipates prior to loss of plasma membrane integrity. We examined $\Delta\Psi$m during necroptosis induced by treatment with TNF plus benzyloxycarbonyl-Val-Ala-DL-Asp-fluoromethylketone (zVAD). We found that loss of $\Delta\Psi$m did not occur until after the plasma membrane became permeable (Figure 1A; Movie S1), suggesting that necroptosis

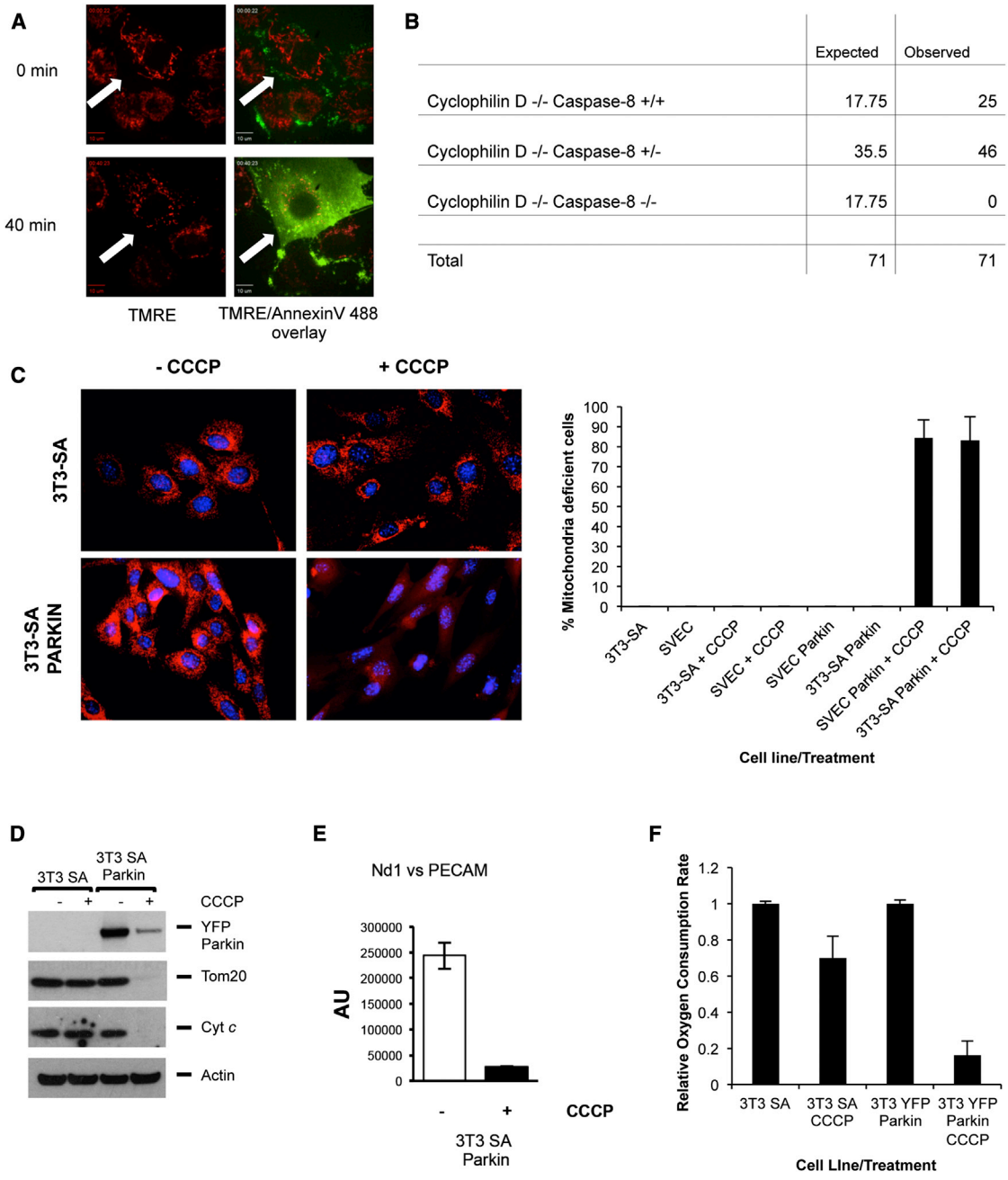

Figure 1. Necroptosis Is Executed Independently of Mitochondrial Permeability Transition

(A) SVEC cells were incubated with TMRE/Annexin V Alexa Fluor 488, treated with TNF+zVAD, and imaged by live-cell confocal microscopy. Images obtained after initial treatment and at the point of cell lysis are shown. Arrow denotes the same cell at different time points.

(B) Expected and observed frequency of caspase-8/cyclophilin D status in offspring from crosses of cyclophilin D −/− caspase 8 +/− mice.

(C) Left: representative images of control or Parkin-expressing 3T3-SA cells treated ± CCCP for 48 hr and immunostained with Tom20 antibody. Right: quantitation of control or Parkin-expressing 3T3-SA or SVEC cells treated ± CCCP for 48 hr that lack mitochondrial Tom20 staining. A minimum of 100 cells were counted per condition per experiment. Error bars represent the SD from the mean of three independent experiments.

(D) Control or Parkin-expressing 3T3-SA cells were treated with CCCP for 48 hr and protein expression was monitored by western blot. Actin was used as a loading control.

(E) Parkin-expressing 3T3-SA cells were treated with CCCP for 48 hr and assayed for mtDNA copy number per nuclear genome. Error bars represent the SD from the mean of triplicate samples. Data are representative of three independent experiments. The same pool of cells was used for the EM analysis shown in Figures 2A and 2B.

(F) Control or Parkin-expressing 3T3-SA cells were treated with CCCP for 48 hr; oxygen consumption was determined and is displayed relative to the untreated control. Error bars represent the SD from the mean of triplicate samples. Data are representative of three independent experiments.

See also Figure S1 and Movie S1.

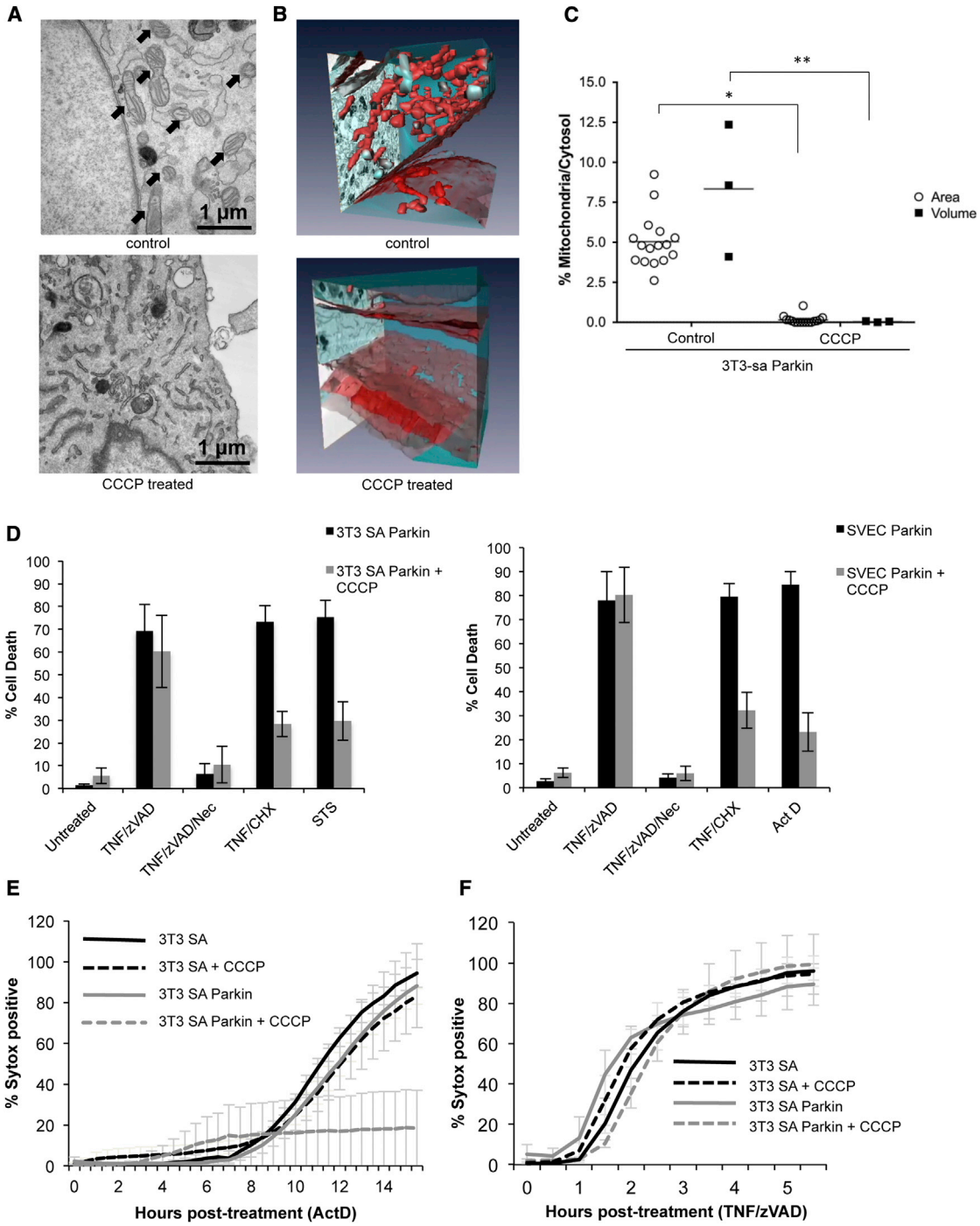

Figure 2. TNF-Dependent Necroptosis Does Not Require Mitochondria

(A) Representative TEM images of control or CCCP-treated 3T3-SA Parkin-expressing cells; arrows denote mitochondria.

(B) Representative 3D-EM images of control or CCCP-treated 3T3-SA Parkin-expressing cells. Mitochondria are colored red and cytosol is colored blue.

(C) 3D-EM quantification of mitochondrial mass of Parkin-expressing 3T3-SA cells treated with CCCP for 48 hr. Black squares represent the area mitochondria/area cytosol ratio, expressed as percentage (% area mitochondria/area cytosol); white circles represent the percentage of the volume mitochondria/volume cytosol ratio. For further information, see Experimental Procedures. *$p < 0.0001$, **$p < 0.05$.

(D) Control or Parkin-expressing 3T3-SA or SVEC cells were treated with CCCP for 48 hr and then treated with the indicated stimuli for 8 hr (TNF+zVAD, TNF+CHX) or overnight with STS or ActD. Cell death was determined by PI positivity and flow cytometry.

(legend continued on next page)

does not require the mitochondrial permeability transition (MPT), which immediately dissipates $\Delta\Psi m$ (Marzo et al., 1998). In support of this finding, and in contrast to RIPK3 deletion, loss of cyclophilin D (a key component of the MPT pore [Baines et al., 2005]) failed to rescue embryonic lethality in Caspase-8 deficient mice (Figure 1B). These and other data (Ch'en et al., 2011) strongly suggest that if mitochondria act as important effectors of necroptosis, they do not do so through the MPT.

To definitively determine the importance of mitochondria as potential effectors in necroptosis, we sought to generate mitochondria-deficient cells. Previous studies have shown that Parkin induces the removal of mitochondria lacking $\Delta\Psi m$ through the process of mitophagy, and that extensive Parkin-mediated mitophagy can fully deplete all mitochondria in a cell (Narendra et al., 2008). We therefore generated SVEC or 3T3-SA cells stably expressing YFP-Parkin and treated them with the protonophore carbonylcyanide *m*-chlorophenylhydrazone (CCCP) for 2 days. Mitochondrial content was assessed by immunostaining for the mitochondrial protein Tom20 (Figure 1C) or by western blotting for the mitochondrial proteins Tom20 and cytochrome *c* (Figures 1D and S1A). A quantitative single-cell analysis demonstrated that at least 80% of the Parkin-expressing, CCCP-treated SVEC or 3T3-SA cells were depleted of mitochondria as evidenced by loss of punctate, mitochondrial Tom20 staining (Figure 1C). A time-course analysis of mitochondrial depletion revealed initial mitochondrial fragmentation followed by aggregation and progressive depletion to below the level of detection (Figure S1B), as in previous studies (Lee et al., 2010; Narendra et al., 2010). Consistent with a penetrant removal of mitochondria, short-term treatment with CCCP completely abolished the clonogenic capacity of Parkin-expressing SVEC and 3T3-SA cells (Figure S1C). We further observed a dramatic loss of mitochondrial cytochrome *c* and Tom20 protein in SVEC Parkin- or 3T3-SA Parkin-expressing cells following CCCP treatment (Figures 1D and S1A). Treated cells were selectively depleted of mtDNA (Figure 1E), lacked oxygen consumption (Figure 1F), and were defective in glutaminolysis (Figure S1D). Mitochondria-deficient cells were viable and persisted in culture for up to several days (Figure S1E), as previously described (Narendra et al., 2008).

TNF-Dependent Necroptosis Does Not Require Mitochondria

To rigorously determine the extent of mitochondrial depletion, we carried out transmission electron microscopy (TEM) and three-dimensional electron microscopy (3D-EM) of Parkin-expressing 3T3-SA cells. CCCP treatment of these cells effectively eliminated mitochondria to undetectable levels (Figures 2A–2C; Movies S2 and S3). It should be noted that although the mitochondria were nearly completely depleted, as assessed by 3D-EM, we nevertheless detected a low level of mtDNA (Figure 1E), which may represent undegraded DNA in lysosomes. These cells were subjected to treatment to induce necroptosis using TNF+zVAD, with or without the RIPK1 inhibitor necrostatin-1 (Nec1), for 8 hr. Despite nearly complete depletion of mitochondria, these cells displayed extensive Nec-1-inhibitable cell death in response to this treatment, as detected by uptake of propidium iodide (PI; 20% versus 21% in control cells without CCCP treatment; data not shown).

3T3-SA or SVEC cells expressing Parkin were then treated with CCCP for 2 days, followed by treatment with TNF+zVAD to induce necroptosis, with or without Nec-1. Alternatively, cells were treated with TNF plus cycloheximide (CHX), staurosporine (STS), or actinomycin D (ActD) to trigger apoptosis. Cell death was measured by PI exclusion. Immunoblotting for cytochrome *c* and Tom20 demonstrated effective removal of mitochondria in Parkin-expressing 3T3-SA or SVEC cells following CCCP treatment (Figures 1D and S1A). Mitochondria-depleted 3T3-SA and SVEC cells expressing Parkin displayed resistance to apoptosis (Figure 2D). Importantly, TNF+zVAD-induced necroptosis occurred to the same extent in both 3T3-SA and SVEC Parkin-expressing cells irrespective of CCCP treatment, and this was inhibited by Nec-1 (Figure 2D). Cell death induced in 3T3-SA cells by TNF+zVAD (necroptosis) or Act D (apoptosis) was then examined by live-cell imaging. Although mitochondria-depleted CCCP-treated 3T3-SA cells expressing Parkin were protected from Act D-induced apoptosis (Figure 2E), the kinetics and extent of necroptosis were identical in 3T3-SA cells expressing Parkin irrespective of CCCP treatment (Figure 2F). Collectively, these data demonstrate that mitochondria are not required for TNF+zVAD-induced necroptosis.

Direct Induction of Programmed Cell Death Demonstrates a Role for Mitochondria in Apoptosis but Not in Programmed Necrosis

To gain a better understanding of the effector mechanisms that act downstream of RIPK3 in programmed necrosis, we constructed a system in which this form of cell death is specifically induced independently of the pleiotropic effects of TNF. We employed inducible dimerization, which uses modified regions of the protein FKBP12 and a rapamycin-derived dimerizer. We generated an induced-active (ac) form of RIPK3 by fusing tandem dimerization domains to the RIPK3 C terminus (Figure 3A). Similarly, an acCaspase-8 was utilized to trigger apoptosis, as described previously (Muzio et al., 1998; Oberst et al., 2010).

To characterize the function of acRIPK3, we stably expressed either full-length murine RIPK3 or acRIPK3 in NIH 3T3 cells, which do not express endogenous RIPK3 (He et al., 2009). The levels of expression of acRIPK3 in these cells and endogenous RIPK3 in 3T3-SA cells appeared similar (Figure S2A). We found that when 3T3 NIH cells expressing either RIPK3 or acRIPK3 were treated with TNF+zVAD, they underwent cell death, which was inhibited by the RIPK1 inhibitor Nec-1 (Figure 3B). However, when treated with dimerizer, acRIPK3-expressing cells

(E) Mitochondria depletion was triggered in 3T3-SA cells by CCCP treatment for 48 hr and cells were treated with ActD as indicated. Cell death was assayed using Sytox Green uptake over time in an IncuCyte imager. Error bars represent the SD from the mean of three independent experiments.
(F) Mitochondria depletion was triggered in 3T3-SA cells by CCCP treatment for 48 hr, and cells were treated with TNF+zVAD as indicated. Cell death was assayed using Sytox Green uptake over time in an IncuCyte imager. Error bars represent the SD from the mean of three independent experiments.
See also Movies S2 and S3.

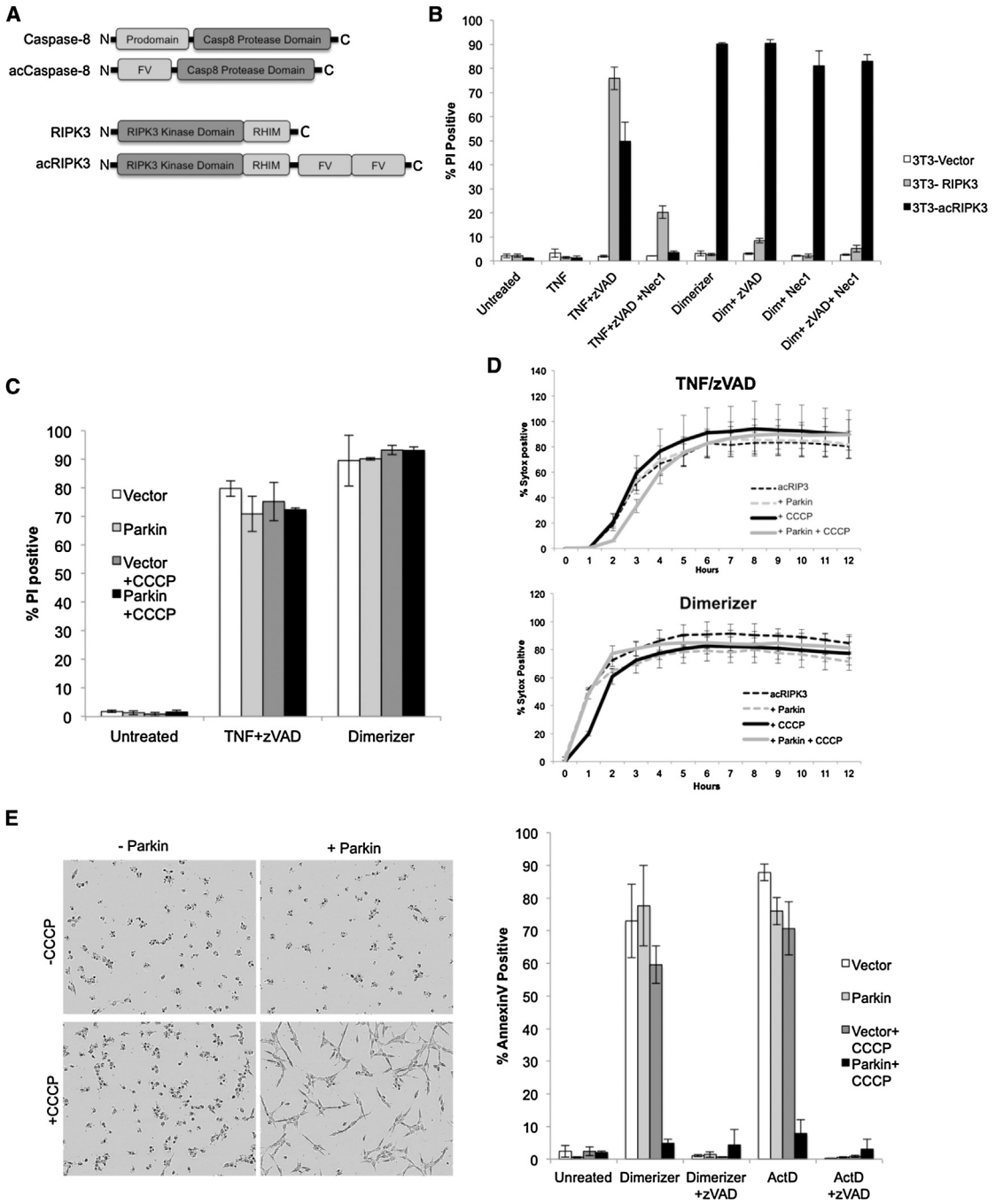

Figure 3. Direct Induction of Programmed Cell Death Demonstrates a Role for Mitochondria in Apoptosis but Not in Programmed Necrosis

(A) Schematic representation of the fusion proteins used to directly induce apoptosis (acCaspase-8) or programmed necrosis (acRIPK3).

(B) NIH 3T3 cells stably transduced with RIPK3 or acRIPK3 were treated as indicated, and cell death was determined by PI positivity and flow cytometry 4 hr later. Error bars represent the SD from the mean of three replicate experiments.

(C) NIH 3T3 cells expressing acRIPK3 and either LZRS vector or Parkin-LZRS were treated with CCCP as indicated to induce elimination of mitochondria. Cell death was induced 48 hr later by the treatments indicated. Error bars represent the SD from the mean of three replicate experiments.

(D) NIH 3T3 cells expressing acRIPK3 were treated to deplete mitochondria, and cell death was quantified with an IncuCyte imager. Sytox-positive cell counts were normalized to total cell numbers using the cell-permeable dye Syto24. Error bars represent the SD from the mean of three independent experiments.

(E) NIH 3T3 cells expressing acCaspase-8 and either LZRS vector or Parkin-LZRS were treated with CCCP as indicated to induce elimination of mitochondria as described in Figure 1. Cell death was induced 48 hr later by the treatments indicated. Left: representative images. Right: the percentage of cells displaying Annexin V positivity was analyzed 8 hr after treatment by flow cytometry. Error bars represent the SD from three replicate experiments.

See also Figure S2.

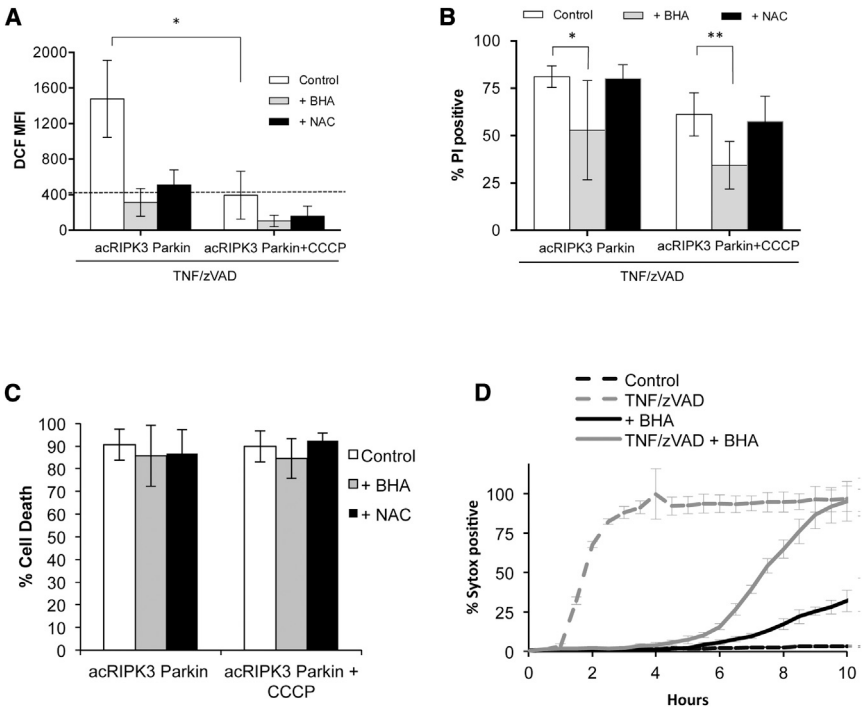

Figure 4. Elimination of Mitochondria Prevents Necroptosis-Associated ROS Production but Does Not Alter RIPK3-Dependent Cell Death

(A) NIH 3T3 cells expressing acRIPK3 and Parkin were treated with CCCP to induce mitochondrial elimination and then treated with TNF+zVAD for 2 hr in the presence of the ROS scavenger BHA or NAC. ROS production was measured using the dye DCF. Results shown are the mean ± SD of $n \geq 3$ independent experiments. *$p < 0.001$. Black dotted line corresponds to the basal level of ROS in the control at t = 0. MFI, mean fluorescent intensity.

(B) NIH 3T3 cells were treated as in (A) for 4 hr and then stained with PI. Cell death was determined by flow cytometry (mean ± SD of $n \geq 3$ independent experiments). *$p < 0.05$, **$p = 0.0518$ (t test).

(C) Mitochondria were depleted as in (A), and RIPK3 dimerization was triggered in the presence of BHA or NAC. Cell death was quantified 2 hr later as in (B) (mean ± SD of $n \geq 3$ independent experiments).

(D) Mitochondria depletion was triggered in NIH 3T3 cells as in (A), and cells were then treated with TNF+zVAD and BHA as indicated. Cell death was measured by Sytox Green uptake over time in an IncuCyte imager. Error bars represent the SD from the mean of triplicate samples. Data are representative of three independent experiments. See also Figure S3.

underwent rapid cell death, whereas RIPK3-expressing cells were unaffected. The cell death observed upon dimerizer-induced activation of acRIPK3 did not require zVAD addition and was not inhibited by Nec-1, consistent with direct activation of RIPK3 by dimerization (Figure 3B).

Mixed lineage kinase like (MLKL) is an essential mediator of RIPK3-dependent necrosis (Sun et al., 2012; Wu et al., 2013; Zhao et al., 2012). Consistent with this role, knockdown of MLKL attenuated TNF+zVAD-induced death of RIPK3-expressing NIH 3T3 cells, and cell death induced by either TNF+zVAD or dimerizer treatment in NIH 3T3 cells expressing acRIPK3 (Figure S2B). AcRIPK3 oligomerization required the kinase activity of RIPK3 to cause necroptosis (Figure S2C), as expected (He et al., 2009). Therefore, RIPK3 oligomerization most likely induces cell death by the same effector mechanism induced by TNF+zVAD.

We next evaluated the effects of depleting mitochondria in cells expressing acCaspase-8 or acRIPK3. Parkin effectively depleted mitochondria in acCaspase-8- or acRIPK3-expressing NIH 3T3 cells (Figures S2D and S2E). We found that upon removal of mitochondria, cell death triggered by either TNF+zVAD or dimerizer was unchanged with respect to extent (Figure 3C) or kinetics (Figure 3D). In contrast, in NIH 3T3 cells stably expressing acCaspase-8, we found that depletion of mitochondria substantially blocked apoptosis-induced dimerizer or ActD treatment (Figure 3E). The requirement for mitochondria in the Caspase-8-induced apoptotic response is consistent with the "type II" response to DR ligation, in which mitochondrial outer membrane permeabilization is required for antagonism of XIAP (Jost et al., 2009).

Roles for the mitochondrial phosphatase PGAM5 and the regulator of mitochondrial fission DRP1 in the execution of necroptosis were recently proposed (Wang et al., 2012). In line with its mitochondrial localization, PGAM5 was effectively depleted from Parkin-expressing cells following CCCP treatment, whereas Drp-1 was unaffected (Figure S2F). However, we failed to observe a role for either protein in our systems (Figure S2). Although knockdown of PGAM5 depleted protein levels (Figure S2G), it did not affect necroptosis induced by TNF or direct activation of acRIPK3 in NIH 3T3 cells (Figure S2H), or in response to TNF+zVAD treatment of 3T3-SA or SVEC cells expressing endogenous RIPK3 (Figure S2J). Furthermore, whereas knockdown of DRP1 (Figure S2G) caused extensive mitochondrial fusion, as expected (Figure S2I), we observed no effect on necroptosis (Figures S2H and S2J). While silencing of these proteins cannot be taken as a formal demonstration that they are not involved in necroptosis, our findings prohibited us from further exploring any possible extramitochondrial roles for PGAM5 or DRP1 in the process.

Elimination of Mitochondria Prevents Necroptosis-Associated ROS Production but Does Not Alter RIPK3-Dependent Cell Death

Investigators have proposed a role for mitochondria in necroptosis largely on the basis of its association with a ROS burst and the finding that the ROS scavenger butylated hydroxyanisole (BHA) effectively delays cell death induced by TNF+zVAD (He et al., 2011; Vanden Berghe et al., 2010). We found that TNF+zVAD induced RIPK3-dependent ROS that was efficiently inhibited by BHA or by another scavenger, N-acetylcysteine (NAC) (Figure 4A). Strikingly, depletion of mitochondria prevented this

ROS burst (Figure 4A). Similar results were found in 3T3-SA cells expressing Parkin (Figure S3B). However, although BHA effectively inhibited necroptosis induced by TNF+zVAD, neither NAC nor mitochondrial depletion influenced cell death (Figures 4B and S3A). This effect of BHA was not observed when necrosis was induced by direct activation of acRIPK3 (Figure 4C). Remarkably, the ability of BHA to partially inhibit necroptosis induced by TNF+zVAD was also observed in cells that were depleted of mitochondria (Figure 4D).

The effect of BHA on necroptosis is therefore independent of mitochondrial ROS, and thus is an "off-target" effect. BHA has been shown to compromise a number of mitochondrial functions in addition to ROS production, including inhibition of Phospholipase-A2 (Festjens et al., 2006), which has also been implicated in necroptosis (Cauwels et al., 2003). However, the failure of BHA to influence necroptosis induced by oligomerization of acRIPK3, and our failure to identify a role for mitochondria in cell death induced by TNF+zVAD or direct activation of RIPK3 suggest that any effects of BHA or other manipulations of mitochondrial functions (Wang et al., 2012) on necroptosis may act upstream of the engagement of RIPK3 activation.

DISCUSSION

Our results strongly argue against a major role for mitochondria as effectors of necroptosis. These findings, as well as the striking rapidity with which RIPK3 activation leads to necrotic death (e.g., Figure S2C), suggest that necroptosis is unlikely to occur via subtle metabolic processes (Zhang et al., 2009) or ROS (Cho et al., 2009). Nevertheless, as roles for necroptosis have been identified in developmental defects (Dillon et al., 2012; Oberst et al., 2011), ischemic injury (Linkermann et al., 2012; Rosenbaum et al., 2010), and other pathologies (He et al., 2009), understanding the way in which RIPK3 mediates its lethal activity remains of great interest.

During early explorations of the mechanisms of apoptosis, it was widely held that the process relied on nuclear events and/or mitochondrial ROS. Important progress was made when it was demonstrated that apoptotic cell death proceeds in cells from which the nuclei have been removed (Jacobson et al., 1994; Schulze-Osthoff et al., 1994) and in cells from which mitochondrial DNA had been depleted (Jacobson et al., 1993). In our studies, we followed a similar logic: if necroptosis is affected by mitochondria, then artificial depletion of mitochondria from a cell should impact the process of necroptosis. Although our studies do not provide a final effector mechanism for this form of cell death, we conclude that efforts to link RIPK3 activation and MLKL to the mitochondria will not be informative for elucidating how cells die by this important process.

EXPERIMENTAL PROCEDURES

Plasmids and Retroviral Transduction

mCherry-Parkin-internal ribosome entry site (IRES)-zeocin and yellow fluorescent protein (YFP)-Parkin-IRES-zeocin were generated by ligating mCherry C1 Parkin and enhanced YFP C1 Parkin (both provided by Dr. Richard Youle) into the LZRS vector (Tait et al., 2010) using standard cloning techniques (see also Supplemental Experimental Procedures).

Microscopy

Live-cell imaging was carried out by spinning-disk confocal microscopy using a Marianas SDC imaging system (for Annexin V/PI/TMRE) or by laser scanning microscopy using a Nikon A1R system for Mitotracker Green (see also Supplemental Experimental Procedures).

RNAi and Western Blot

Cells (5×10^4) were transfected with control or Smartpool RNAi duplexes (Dharmacon) targeting murine MLKL, PGAM5, or Drp-1. Duplexes were transfected twice on consecutive days with Lipofectamine 2000 (Invitrogen) according to the manufacturer's instructions. Cells were analyzed 3 days after the initial transfection (see also Supplemental Experimental Procedures).

Clonogenicity Assay, Treatments, and Cell Death Assays

Cells were seeded in 12-well plates (5×10^3 cells per well) and left untreated or treated with CCCP (12.5 μM) two times over a 24 hr period, after which time it was washed out and replaced with complete media. Colonies were stained with methylene blue solution (1% w/v methylene blue in a 50:50 methanol/water solution; see also Supplemental Experimental Procedures).

Seahorse Oxygen Consumption Assay, mtDNA, and ROS Quantification

Respiration was measured with a Seahorse XF24 analyzer. Cells were seeded in plates coated with poly-L-lysine. After 5 hr, the cells were loaded into the machine to determine the oxygen consumption rate (see also Supplemental Experimental Procedures).

Generation of cyclophilinD-ko/caspase-8 het Mice and Statistical Analysis

To generate cyclophilinD-KO/caspase-8 HET mice, we crossed cyclophilin D-KO mice (B6;129-Ppif tm1Jmol/J, order no. 009071; The Jackson Laboratory; described in Nakayama et al., 2007) with caspase-8/RIPK3-DKO mice (Oberst et al., 2011; see also Supplemental Experimental Procedures).

SUPPLEMENTAL INFORMATION

Supplemental Information includes Supplemental Experimental Procedures, three figures, and three movies and can be found with this article online at http://dx.doi.org/10.1016/j.celrep.2013.10.034.

ACKNOWLEDGMENTS

We thank Drs. Richard Youle and Jacques Neefjes for reagents, and Linda Horner, Velita Thornton, Margaret O'Prey, and Olivia Lombardi for technical support. This work was funded by the Royal Society and grants from the BBSRC (BB/K008374/1) (S.W.G.T.) grants AI44828 and CA169291 from the NIH (to D.R.G.), and the American Lebanese and Syrian Associated Charities. S.W.G.T. is a Royal Society University Research Fellow.

Received: August 20, 2013
Revised: October 2, 2013
Accepted: October 21, 2013
Published: November 21, 2013

REFERENCES

Baines, C.P., Kaiser, R.A., Purcell, N.H., Blair, N.S., Osinska, H., Hambleton, M.A., Brunskill, E.W., Sayen, M.R., Gottlieb, R.A., Dorn, G.W., et al. (2005). Loss of cyclophilin D reveals a critical role for mitochondrial permeability transition in cell death. Nature *434*, 658–662.

Cauwels, A., Janssen, B., Waeytens, A., Cuvelier, C., and Brouckaert, P. (2003). Caspase inhibition causes hyperacute tumor necrosis factor-induced shock via oxidative stress and phospholipase A2. Nat. Immunol. *4*, 387–393.

Ch'en, I.L., Tsau, J.S., Molkentin, J.D., Komatsu, M., and Hedrick, S.M. (2011). Mechanisms of necroptosis in T cells. J. Exp. Med. *208*, 633–641.

Cho, Y.S., Challa, S., Moquin, D., Genga, R., Ray, T.D., Guildford, M., and Chan, F.K. (2009). Phosphorylation-driven assembly of the RIP1-RIP3 complex regulates programmed necrosis and virus-induced inflammation. Cell *137*, 1112–1123.

Dillon, C.P., Oberst, A., Weinlich, R., Janke, L.J., Kang, T.B., Ben-Moshe, T., Mak, T.W., Wallach, D., and Green, D.R. (2012). Survival function of the FADD-CASPASE-8-cFLIP(L) complex. Cell reports *1*, 401–407.

Festjens, N., Kalai, M., Smet, J., Meeus, A., Van Coster, R., Saelens, X., and Vandenabeele, P. (2006). Butylated hydroxyanisole is more than a reactive oxygen species scavenger. Cell Death Differ. *13*, 166–169.

Goldstein, J.C., Waterhouse, N.J., Juin, P., Evan, G.I., and Green, D.R. (2000). The coordinate release of cytochrome c during apoptosis is rapid, complete and kinetically invariant. Nat. Cell Biol. *2*, 156–162.

Green, D.R., Oberst, A., Dillon, C.P., Weinlich, R., and Salvesen, G.S. (2011). RIPK-dependent necrosis and its regulation by caspases: a mystery in five acts. Mol. Cell *44*, 9–16.

He, S., Wang, L., Miao, L., Wang, T., Du, F., Zhao, L., and Wang, X. (2009). Receptor interacting protein kinase-3 determines cellular necrotic response to TNF-alpha. Cell *137*, 1100–1111.

He, S., Liang, Y., Shao, F., and Wang, X. (2011). Toll-like receptors activate programmed necrosis in macrophages through a receptor-interacting kinase-3-mediated pathway. Proc. Natl. Acad. Sci. USA *108*, 20054–20059.

Jacobson, M.D., Burne, J.F., King, M.P., Miyashita, T., Reed, J.C., and Raff, M.C. (1993). Bcl-2 blocks apoptosis in cells lacking mitochondrial DNA. Nature *361*, 365–369.

Jacobson, M.D., Burne, J.F., and Raff, M.C. (1994). Programmed cell death and Bcl-2 protection in the absence of a nucleus. EMBO J. *13*, 1899–1910.

Jost, P.J., Grabow, S., Gray, D., McKenzie, M.D., Nachbur, U., Huang, D.C., Bouillet, P., Thomas, H.E., Borner, C., Silke, J., et al. (2009). XIAP discriminates between type I and type II FAS-induced apoptosis. Nature *460*, 1035–1039.

Kim, Y.S., Morgan, M.J., Choksi, S., and Liu, Z.G. (2007). TNF-induced activation of the Nox1 NADPH oxidase and its role in the induction of necrotic cell death. Mol. Cell *26*, 675–687.

Lee, J.Y., Nagano, Y., Taylor, J.P., Lim, K.L., and Yao, T.P. (2010). Disease-causing mutations in parkin impair mitochondrial ubiquitination, aggregation, and HDAC6-dependent mitophagy. J. Cell Biol. *189*, 671–679.

Lin, Y., Choksi, S., Shen, H.M., Yang, Q.F., Hur, G.M., Kim, Y.S., Tran, J.H., Nedospasov, S.A., and Liu, Z.G. (2004). Tumor necrosis factor-induced nonapoptotic cell death requires receptor-interacting protein-mediated cellular reactive oxygen species accumulation. J. Biol. Chem. *279*, 10822–10828.

Linkermann, A., Bräsen, J.H., Himmerkus, N., Liu, S., Huber, T.B., Kunzendorf, U., and Krautwald, S. (2012). Rip1 (receptor-interacting protein kinase 1) mediates necroptosis and contributes to renal ischemia/reperfusion injury. Kidney Int. *81*, 751–761.

Marzo, I., Brenner, C., Zamzami, N., Susin, S.A., Beutner, G., Brdiczka, D., Rémy, R., Xie, Z.H., Reed, J.C., and Kroemer, G. (1998). The permeability transition pore complex: a target for apoptosis regulation by caspases and bcl-2-related proteins. J. Exp. Med. *187*, 1261–1271.

Muzio, M., Stockwell, B.R., Stennicke, H.R., Salvesen, G.S., and Dixit, V.M. (1998). An induced proximity model for caspase-8 activation. J. Biol. Chem. *273*, 2926–2930.

Nakayama, H., Chen, X., Baines, C.P., Klevitsky, R., Zhang, X., Zhang, H., Jaleel, N., Chua, B.H., Hewett, T.E., Robbins, J., et al. (2007). Ca2+- and mitochondrial-dependent cardiomyocyte necrosis as a primary mediator of heart failure. J. Clin. Invest. *117*, 2431–2444.

Narendra, D., Tanaka, A., Suen, D.F., and Youle, R.J. (2008). Parkin is recruited selectively to impaired mitochondria and promotes their autophagy. J. Cell Biol. *183*, 795–803.

Narendra, D., Kane, L.A., Hauser, D.N., Fearnley, I.M., and Youle, R.J. (2010). p62/SQSTM1 is required for Parkin-induced mitochondrial clustering but not mitophagy; VDAC1 is dispensable for both. Autophagy *6*, 1090–1106.

Oberst, A., Pop, C., Tremblay, A.G., Blais, V., Denault, J.B., Salvesen, G.S., and Green, D.R. (2010). Inducible dimerization and inducible cleavage reveal a requirement for both processes in caspase-8 activation. J. Biol. Chem. *285*, 16632–16642.

Oberst, A., Dillon, C.P., Weinlich, R., McCormick, L.L., Fitzgerald, P., Pop, C., Hakem, R., Salvesen, G.S., and Green, D.R. (2011). Catalytic activity of the caspase-8-FLIP(L) complex inhibits RIPK3-dependent necrosis. Nature *471*, 363–367.

Rosenbaum, D.M., Degterev, A., David, J., Rosenbaum, P.S., Roth, S., Grotta, J.C., Cuny, G.D., Yuan, J., and Savitz, S.I. (2010). Necroptosis, a novel form of caspase-independent cell death, contributes to neuronal damage in a retinal ischemia-reperfusion injury model. J. Neurosci. Res. *88*, 1569–1576.

Schulze-Osthoff, K., Walczak, H., Dröge, W., and Krammer, P.H. (1994). Cell nucleus and DNA fragmentation are not required for apoptosis. J. Cell Biol. *127*, 15–20.

Sun, L., Wang, H., Wang, Z., He, S., Chen, S., Liao, D., Wang, L., Yan, J., Liu, W., Lei, X., and Wang, X. (2012). Mixed lineage kinase domain-like protein mediates necrosis signaling downstream of RIP3 kinase. Cell *148*, 213–227.

Tait, S.W., Parsons, M.J., Llambi, F., Bouchier-Hayes, L., Connell, S., Muñoz-Pinedo, C., and Green, D.R. (2010). Resistance to caspase-independent cell death requires persistence of intact mitochondria. Dev. Cell *18*, 802–813.

Vanden Berghe, T., Vanlangenakker, N., Parthoens, E., Deckers, W., Devos, M., Festjens, N., Guerin, C.J., Brunk, U.T., Declercq, W., and Vandenabeele, P. (2010). Necroptosis, necrosis and secondary necrosis converge on similar cellular disintegration features. Cell Death Differ. *17*, 922–930.

Vanlangenakker, N., Vanden Berghe, T., Bogaert, P., Laukens, B., Zobel, K., Deshayes, K., Vucic, D., Fulda, S., Vandenabeele, P., and Bertrand, M.J. (2011). cIAP1 and TAK1 protect cells from TNF-induced necrosis by preventing RIP1/RIP3-dependent reactive oxygen species production. Cell Death Differ. *18*, 656–665.

Wang, Z., Jiang, H., Chen, S., Du, F., and Wang, X. (2012). The mitochondrial phosphatase PGAM5 functions at the convergence point of multiple necrotic death pathways. Cell *148*, 228–243.

Wu, J., Huang, Z., Ren, J., Zhang, Z., He, P., Li, Y., Ma, J., Chen, W., Zhang, Y., Zhou, X., et al. (2013). Mlkl knockout mice demonstrate the indispensable role of Mlkl in necroptosis. Cell Res. *23*, 994–1006.

Zhang, D.W., Shao, J., Lin, J., Zhang, N., Lu, B.J., Lin, S.C., Dong, M.Q., and Han, J. (2009). RIP3, an energy metabolism regulator that switches TNF-induced cell death from apoptosis to necrosis. Science *325*, 332–336.

Zhao, J., Jitkaew, S., Cai, Z., Choksi, S., Li, Q., Luo, J., and Liu, Z.G. (2012). Mixed lineage kinase domain-like is a key receptor interacting protein 3 downstream component of TNF-induced necrosis. Proc. Natl. Acad. Sci. USA *109*, 5322–5327.